Journal of Anatomy

J. Anat. (2019) doi: 10.1111/joa.13115

Development and growth of the pectoral girdle and fin skeleton in the extant coelacanth *Latimeria chalumnae*

Rohan Mansuit,[1,2] Gaël Clément,[1] Anthony Herrel,[2] Hugo Dutel,[3] Paul Tafforeau,[4] Mathieu D. Santin[5] and Marc Herbin[2]

[1]*UMR 7207 Centre de Recherche en Paléontologie, Paris, MNHN – Sorbonne Université – CNRS, Département Origines & Evolution, Muséum national d'Histoire naturelle, Paris, France*
[2]*UMR 7179 MECADEV, MNHN – CNRS, Département Adaptations du Vivant, Muséum National d'Histoire Naturelle, Paris, France*
[3]*School of Earth Sciences, University of Bristol, Bristol,, UK*
[4]*European Synchrotron Radiation Facility, Grenoble Cedex, France*
[5]*Inserm U 1127, CNRS UMR 7225, Centre for NeuroImaging Research, ICM (Brain & Spine Institute), Sorbonne University, Paris, France*

Abstract

The monobasal pectoral fins of living coelacanths and lungfishes are homologous to the forelimbs of tetrapods and are thus critical to investigate the origin thereof. However, it remains unclear whether the similarity in the asymmetrical endoskeletal arrangement of the pectoral fins of coelacanths reflects the evolution of the pectoral appendages in sarcopterygians. Here, we describe for the first time the development of the pectoral fin and shoulder girdle in the extant coelacanth *Latimeria chalumnae*, based on the tomographic acquisition of a growth series. The pectoral girdle and pectoral fin endoskeleton are formed early in development with a radially outward growth of the endoskeletal elements. The visualization of the pectoral girdle during development shows a reorientation of the girdle between the fetus and pup 1 stages, creating a contact between the scapulocoracoids and the clavicles in the ventro-medial region. Moreover, we observed a splitting of the pre- and post-axial cartilaginous plates in respectively pre-axial radials and accessory elements on one hand, and in post-axial accessory elements on the other hand. However, the mechanisms involved in the splitting of the cartilaginous plates appear different from those involved in the formation of radials in actinopterygians. Our results show a proportional reduction of the proximal pre-axial radial of the fin, rendering the external morphology of the fin more lobe-shaped, and a spatial reorganization of elements resulting from the fragmentation of the two cartilaginous plates. *Latimeria* development hence supports previous interpretations of the asymmetrical pectoral fin skeleton as being plesiomorphic for coelacanths and sarcopterygians.

Key words: Actinistia; endoskeleton; fin; ontogeny; pectoral girdle; sarcopterygian; tomography.

Introduction

Among the sarcopterygians, the clade Actinistia is today only represented by the coelacanth genus *Latimeria,* and is considered as the sister group to the Rhipidistia, represented by living lungfishes and tetrapods (Ahlberg, 1991; Forey, 1998; Friedman et al., 2007; Clack, 2012; Amemiya et al., 2013). This clade presents a long evolutionary history with its origin dating back to the Early Devonian (Johanson et al., 2006; Friedman, 2007; Zhu et al., 2012b). Coelacanths are well represented in the fossil record, with about 40 described genera and more than 130 species (Forey, 1998). The clade also presents an important diversity of form, size and ecology (Forey, 1998; Friedman & Coates, 2006; Casane & Laurenti, 2013; Cavin & Guinot, 2014; Cavin et al., 2017), and was considered to have become extinct at the end of the Mesozoic era (Smith, 1939). Today, there are two known species: *Latimeria chalumnae* (Smith, 1939) in the western Indian Ocean and *L. menadoensis* (Erdmann et al., 1998; Pouyaud et al., 1999), discovered offshore of Sulawesi, Indonesia.

Because of their close relationships with tetrapods, many aspects of the biology and development of the coelacanths are of interest to better understand the

Correspondence
Rohan Mansuit, UMR 7179 MECADEV, MNHN – CNRS, Département Adaptations du Vivant, 55 rue Buffon, 75005 Paris, France.
E: rohan.mansuit@mnhn.fr

Accepted for publication *10 October 2019*

origin, the anatomical characteristics and the evolution of osteichthyans (Dutel et al., 2019) and early land vertebrates (Fricke & Hissmann, 1992). Pectoral fins of coelacanths are moreover of particular interest, partly because the paired fin skeleton of the coelacanth is organized along a metapterygial axis (Millot & Anthony, 1958). This organization is similar to that of the endochondral skeletal elements of lungfishes and tetrapod limbs (Shubin & Alberch, 1986; Mabee, 2000). Consequently, the paired lobed-fin of sarcopterygian fishes is considered homologous to the tetrapod limb (i.e. Gregory & Raven, 1941; Westoll, 1943; Fricke & Hissmann, 1992; Clack, 2009). Moreover, the first elements of the pectoral fin of the coelacanth (the first mesomere, the first pre-axial radial and the second mesomere) are considered to be homologous to the stylopodal and zeugopodal elements of the tetrapod limb (Fricke & Hissmann, 1992; Johanson et al., 2007; Miyake et al., 2016). The majority of studies concerning the water-to-land transition of vertebrates have focused on the pectoral appendages given their importance during locomotion in transitional and early terrestrial vertebrates (Shubin et al., 2006; Pierce et al., 2012; Standen et al., 2014). Coelacanths have also been considered to be relevant in the context of terrestrialization because they move their fins in an alternating manner, reminiscent of the movements of tetrapod limbs (Fricke et al., 1987; Forey, 1998; Clack, 2012). However, the fins of the extant coelacanth clearly do not function as 'legs', i.e. crawl on sea bottom, as had been supposed by Smith (1956). Whereas lungfishes are more closely related to tetrapods than coelacanths, as early as the beginning of their evolutionary history, they present modified paired fins with a high degree of symmetry that do not reflect the pectoral fin of early sarcopterygians (Ahlberg, 1989; Coates et al., 2002; Coates, 2003; Friedman et al., 2007). One the other hand, early tetrapodomorphs and coelacanths show asymmetrical fins (Ahlberg, 1989; Friedman et al., 2007), where the pre-axial and post-axial side of the fin do not have the same arrangement around the metapterygial axis. It remains unknown, however, whether the evolution of the pectoral fin of coelacanths is informative about the evolution of the pectoral appendages in sarcopterygians more generally.

The pectoral fin and girdle development of the living coelacanth remains unknown. Consequently, a detailed anatomical description of the morphology and anatomy of the pectoral fin and girdle at different ontogenetic stages of the extant coelacanth is crucial for an understanding of the development of the pectoral fin of *Latimeria* in comparison with fossil coelacanths and tetrapodomorphs. The development of the endoskeleton of the pectoral fin and girdle in *Latimeria* is likely to be informative for reconstructing the plesiomorphic configuration of the pectoral appendages in sarcopterygians (Coates et al., 2002; Amaral & Schneider, 2017). Here, we study the development of the pectoral fin and girdle in the extant coelacanth by describing this anatomical complex in a unique ontogenetic series of five stages comprised of three prenatal stages and two post-natal stages (Dutel et al., 2019).

Materials and methods

Specimens

The developmental series includes five stages from several museum collections (Fig. 1). The first stage is a fetus of 5 cm total length (TL; CCC 202.1) (Nulens et al., 2011) found inside the female specimen CCC 202 captured off the Tanzanian coast in 2005 and conserved in the collection of the South African Institute for Aquatic Biodiversity, Grahamstown, South Africa (SAIAB 76199). Stage 2 is a pup of 32.3 cm TL with a yolk sac (CCC 29.5) found inside the female specimen CCC 29 captured off the Comores Island in 1969 and conserved in the collection of the MNHN, Paris, France (MNHN AC 2012-22). Stage 3 is a late pup of 34.8 cm TL (CCC 162.21) with a resorbed yolk sac, found inside the female CCC 162 captured off the coast of Mozambique in 1991 and conserved in the collection of the Zoologische Staatssammlung, Munich, Germany (ZSM 28409). Stage 4 is a juvenile of 42.5 cm TL (CCC 94) captured off Grande Comore in 1974 and conserved in the collection of the MNHN, Paris, France (MNHN AC 2012-27). The adult specimen (stage 5) principally used in this study is a male of 130 cm TL (CCC 22) captured in Grande Comore in 1960 and conserved in the collection of the MNHN, Paris, France (MNHN AC 2012-18). Direct anatomical observations were also made on isolated pectoral fin skeletons of several adult specimens: CCC 6 (MNHN AC 2012-4), CCC 7 (MNHN AC 2012-5), CCC 14 (MNHN AC 2012-11) and CCC 19 (MNHN AC 2012-15). Specimens from the MNHN, Paris, are preserved in a 6–7% formaldehyde solution, and the others are preserved in a 70% aqueous ethanol solution.

Imaging

Stage 1 – Fetus (CCC 202.1)

The specimen was scanned using long propagation phase-contrast synchrotron X-ray microtomography at the ID19 beamline of the European Synchrotron Radiation Facility (ESRF), Grenoble (France). It was imaged at a voxel size 6.5 μm using a pink beam achieved with a W150 wiggler at a gap of 50 mm and filtered with 2 mm aluminium, 0.25 mm copper and 0.2 mm gold. The scintillator was a 250-μm-thick LuAG:Ce (lutetium–aluminium–garnet) crystal. The resulting detected spectrum was centred on 73 keV with a bandwidth of 17 keV FWHM (full width at half maximum). The detector was a FreLoN 2K14 charge coupled device (CCD) camera mounted on a lens system. To obtain a sufficient propagation phase-contrast effect, a distance of 3 m between the sample and the detector was used. The final reconstruction (13 μm) was obtained after binning with the software ImageJ.

Stage 2 – Pup 1 (with yolk sac) (CCC 29.5)

The specimen was scanned using long propagation phase-contrast synchrotron X-ray microtomography at the ID19 beamline of the European Synchrotron Radiation Facility (ESRF), Grenoble (France). It was scanned at a voxel size of 23.34 μm and using a propagation distance of 13 m to maximize the phase-contrast effect. The beam produced by the ID19 W150 wiggler at a gap of 59 mm was filtred

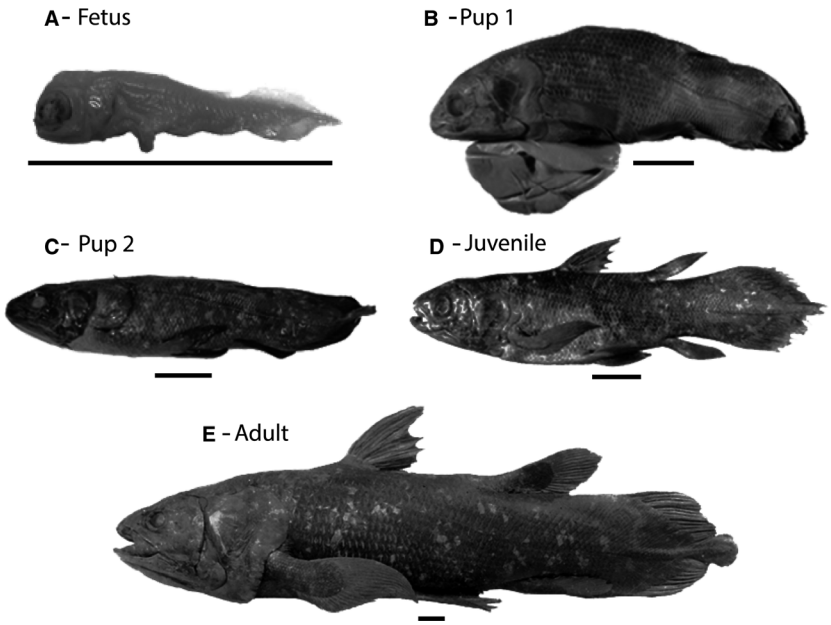

Fig. 1 *Latimeria chalumnae* – Ontogenetic series in left lateral view. (A) Fetus (CCC 202.1). (B) First pup (CCC 29.5). (C) Second pup (CCC 162.21). (D) Juvenile (CCC 94). (E) Adult (CCC 22). Scale bar: 5 cm.

through 2.8 mm aluminium and 1.4 mm copper, resulting in an average detected energy of 77.4 keV. The scintillator was a 2000-μm-thick LuAG:Ce crystal. The detector was a PCO edge 4.2 sCMOS. The final reconstruction (46.68 μm) was obtained after binning with the software ImageJ.

Stage 3 – Pup 2 (with resorbed yolk sac) (CCC 162.21)

The specimen was scanned using long propagation phase-contrast synchrotron X-ray microtomography at the ID19 beamline of the European Synchrotron Radiation Facility (ESRF), Grenoble (France). It was scanned at a voxel size of 30.45 μm using the ID19 W150 wiggler at a gap of 50 mm filtered by 2 mm aluminium, 0.25 mm copper and 0.25 mm tungsten. The scintillator, detector and distance between the sample and the detector were the same as for the fetus. The final reconstruction (60.90 μm) was obtained after binning in ImageJ.

Stage 4 – Juvenile (CCC 94)

The specimen was scanned twice, once at the ESRF (Grenoble, France) and once using an MRI scan at the ICM (Paris, France). At the ESRF, the specimen was scanned at a voxel size of 28.43 μm and using a propagation distance of 13 m to maximize the phase-contrast effect. The beam produced by the ID19 W150 wiggler at a gap of 30 mm was filtered by 2 mm aluminium and 15 mm copper, resulting in an average detected energy of 170 keV with a bandwidth of 85 keV FWHM. The detector camera was a FreLoN 2K charge coupled device mounted on a lens system composed of a 750-mm-thick LuAG:Ce scintillator. The final reconstruction (56.86 μm) was obtained after binning in ImageJ, and was used for the 3D-rendering of the pectoral girdle. As the contrast was not excellent, possibly due to a historical treatment by injection of a colloidal barite solution (Anthony, 1980), the specimen was re-scanned with magnetic resonance imaging (MRI) at the Centre for Neuroimaging Research, ICM (Brain & Spine Institute). MRI was performed at 3T with a Siemens Tim TRIO (Siemens, Germany) system. Images were acquired with a 3D Flash sequence with an isotropic resolution of 300 μm. Parameters were: Matrix size = 640*300*256; TR/TE (ms) = 18/4.73; Flip Angle = 10°; Spectral Width = 100 kHz; Number of averages = 20; Total acquisition time was 7 h and 41 min. The RMI data were used for the 3D-rendering of the pectoral fin endoskeleton.

Synchrotron data were reconstructed using a filtered back-projection algorithm coupled with a single distance phase-retrieval process (Paganin et al., 2002; Sanchez et al., 2012). For each sample, all the sub-scans were reconstructed separately, converted into 16-bit TIFF stacks and then concatenated to generate a single complete scan of each specimen. The ring artefacts were corrected on the reconstructed slices using a specific tool developed at the European Synchrotron Radiation Facility (Lyckegaard et al., 2011).

Stage 5 – Adult (CCC 22)

The specimen CCC 22 was scanned with a high-resolution computerized axial tomography scanning (CAT scan) in a Parisian hospital (France) using the following scanning parameters: effective energy 120 kV, current 158 mA, voxel size 742 μm and 1807 views.

The slices were reconstructed and exported into 16-bit TIFF stacks using the Phoenix datos|× 2.0 reconstruction software, and exported into 16-bit TIFF stacks.

Segmentation and 3D-reconstruction method

For all the specimens, segmentation and 3D rendering were done using the software mimics Innovation Suite 20.0 (Materialise).

Results

The pectoral girdle

In the adult, the pectoral girdle is composed of four flattened and elongated dermal bones – the clavicle, the cleithrum, the anocleithrum and the extracleithrum – and one endochondral bone, the scapulocoracoid as described by Millot & Anthony (1958) (Fig. 2). The girdle forms an arc posterior to the branchial arches. As the general

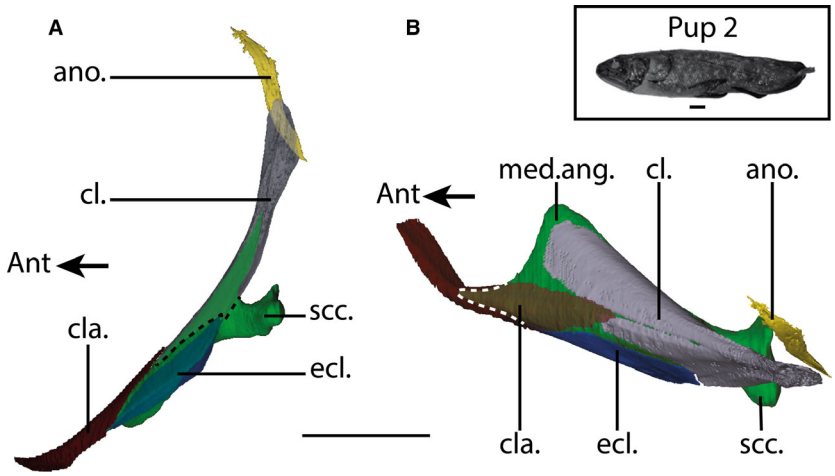

Fig. 2 *Latimeria chalumnae* – Second pup. Left pectoral girdle in lateral (A) and dorsal (B) view. The cleithrum and extracleithrum are transparent in (A), revealing the general shape of the scapulocoracoid. The clavicle is transparent in (B), revealing the lateral angle of the scapulocoracoid. The dotted line shows the edge of the cleithrum in (A) and the edge of the scapulocoracoid in (B). ano., anocleithrum; cl., cleithrum; cla., clavicle; ecl., extracleithrum; lat.ang., lateral angle of the scapulocoracoid; med.ang., medial angle of the scapulocoracoid; scc., scapulocoracoid. Scale bar: 20 mm.

morphlogy of the pectoral girdle does not change between the different stages, our illustrations depict pup 2 only (Fig. 2).

The pectoral girdle is already well developed in the fetus and does not change dramatically in the four successive stages (Fig. 3). Indeed, the bones continue to grow, but conserve their general shape. However, there is a shift in orientation of the complete pectoral complex (Fig. 4) between the fetus and pup 1. In the fetus, the medial margin of the girdle is oriented toward the ventral side of the embryo, there is no contact between the anterior part of the right and left girdles, and the extracleithrum has a dorsal position on the scapulocoracoid. In pup 1, the medial margin of the girdle rotates in a dorsal direction, leading to the contact between their two anterior extremities, also observed in the following stages, and the extracleithrum has a more lateral position on the scapulocoracoid (Fig. 4). In the juvenile, the cleithrum, extracleithrum and clavicle of the pectoral girdle move progressively closer to one another. In the adult stage, these three bones are in close contact with one another, with the edges of the bones overlapping. On the μCT scan, the three bones appear fused; however, this may be due to the limited resolution of the scan. Indeed, the observation of isolated pectoral girdles shows that the three bones are not fused and that each bone is independent.

- The anocleithrum (ano.)

The anocleithrum is the most dorsal bone of the pectoral girdle, closely located, but without contact, to the medial side of the dorsal end of the cleithrum. It is a small, flat and straight bone, oriented dorso-ventrally. The anocleithrum is attached to the cleithrum by a ligament, as described previously by Millot & Anthony (1958). The general morphology of this dermal bone changes dramatically during development.

In the fetus, the anocleithrum is straight and proportionally smaller compared with other stages (Fig. 3). In lateral view, it extends beyond the antero-dorsal margin of the dorsal end of the cleithrum. In pup 1, the anocleithrum is proportionally longer, and is gently curved to follow the lateral body surface. It also extends beyond the antero-dorsal margin of the dorsal end of the cleithrum. From pup 2 onwards, it extends beyond both the antero-dorsal and postero-ventral margins of the dorsal end of the cleithrum (Fig. 5).

The anocleithrum shows some individual variability and asymmetry. Pup 1 has a right anocleithrum with a convex shape in anterior direction, whereas the left one is straight (Fig. 5A). In pup 2, the left anocleithrum is S-shaped, whereas the right one is straighter (Fig. 5B). The right anocleithrum of the adult is bifid with a backward pointing process, whereas the left one is straight (Fig. 5D). This condition was previously noticed by Millot & Anthony (1958) in another adult specimen (MNHN AC-2012-1 = CCC 3).

- The cleithrum (cl.)

In the adult, the cleithrum is an elongated bone fused with the extracleithrum and the clavicle, overlapping the dorsal surface of the scapulocoracoid (Fig. 2). The medial margin of the cleithrum forms a gutter to accommodate the medial margin of the scapulocoracoid. The cleithrum contacts the extracleithrum at its lateral edge, and in its posterior part forms a gutter surrounding the lateral margin of the scapulocoracoid until the level of the articular process of the scapulocoracoid. The dorsal part of the cleithrum surrounds the dorsal tip of the scapulocoracoid. The uppermost part of the cleithrum is flattened latero-medially and flared dorso-ventrally, with a more or less pronounced longitudinal ridge on the lateral side of the bone. In the fetus, the dorsal lamina of the cleithrum is dorso-medially oriented. Its dorsal tip is pointed and its anterior margin slightly convex (Fig. 3). In later stages, the dorsal tip is spatula-shaped and the anterior margin tends to be progressively more concave (Fig. 3).

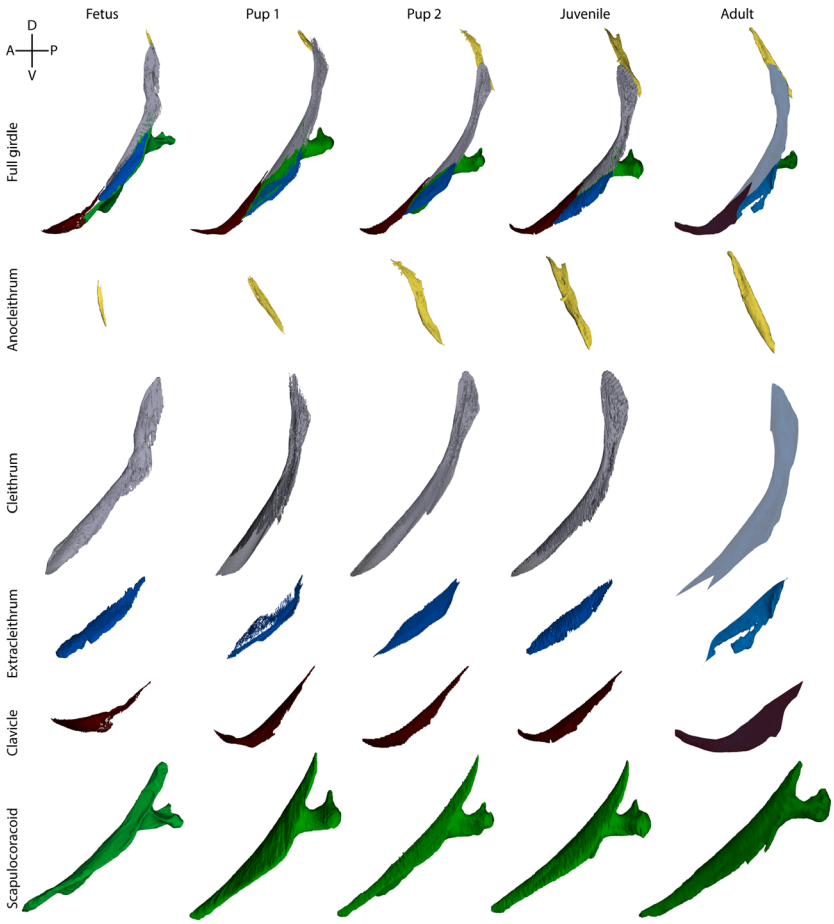

Fig. 3 *Latimeria chalumnae*. Elements of the left pectoral girdle in lateral view at five different developmental stages (1–5). The different stages are not to scale, but the different bones within a given stage are to scale.

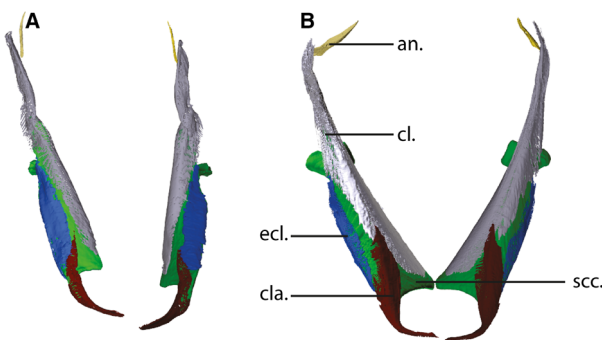

Fig. 4 *Latimeria chalumnae* – The fetus and the first pup. Anterior views of the pectoral girdles of the fetus (A) and first pup (B), illustrating the reorientation of the pectoral girdles during the development of the coelacanth. cl., cleithrum; cla., clavicle; ecl., extracleithrum; scc., scapulocoracoid. Not to scale.

- The extracleithrum (ecl.)

The extracleithrum has an elongated diamond shape and its lateral margin extends lower than the lateral margin of the scapulocoracoid (Fig. 2). Its postero-medial edge contacts the cleithrum and its antero-medial margin is overlapped by the clavicle. The scapulocoracoid fits in the gutter-shaped internal side of the lateral margin of the extracleithrum (Fig. 2). In the fetus, the lateral margin of the extracleithrum simply follows the lateral margin of the scapulocoracoid. The gutter-type contact present in later stages is not formed yet.

The extracleithrum is separated from the clavicle by a gap that decreases during the development and disappears from the juvenile onwards. In pup 1, the lateral margin of the extracleithrum extends beyond the lateral margin of the scapulocoracoid and a long gutter appears on its internal side from pup 2 onwards.

- The clavicle (cla.)

In the adult, the enlarged posterior part of the clavicle is positioned at the antero-lateral part of the scapulocoracoid (Fig. 2). In cross-section, it appears that the posterior tip of the clavicle overlaps the margins of the cleithrum and extracleithrum (Fig. 6). The medial and lateral margins of the clavicle form two gutters that the lateral angle of the scapulocoracoid fits into, then extends antero-ventrally as a twisted shank (Fig. 2). This shank is horizontal, medially concave and reaches the median plane of the ventral side of the body. According to Millot & Anthony (1958), both twisted shanks articulate with a narrow basal lamina,

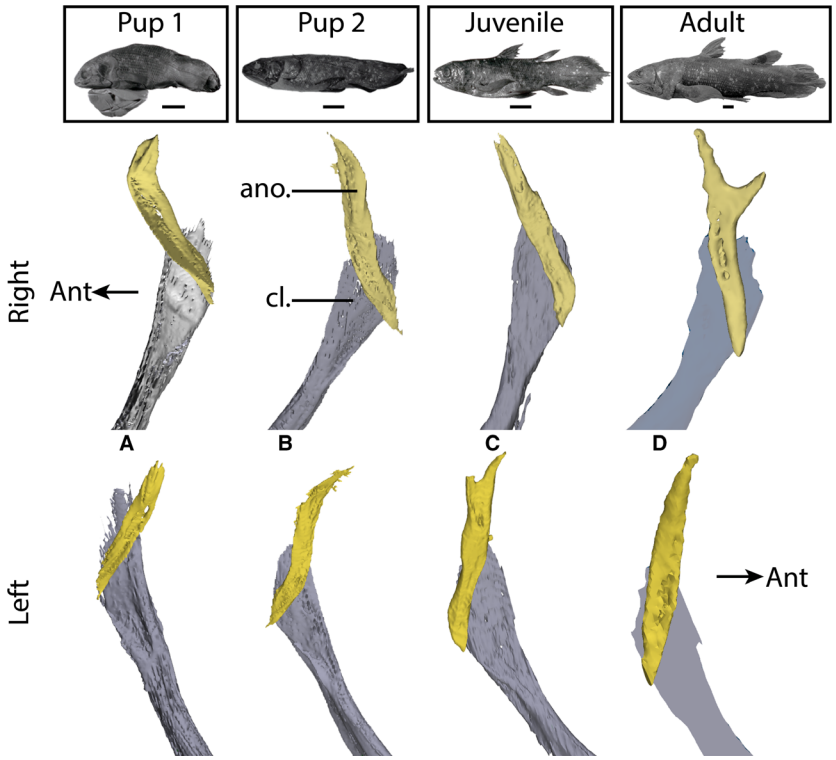

Fig. 5 *Latimeria chalumnae* – Stages 2–5. Right anocleithrum (top) and left anocleithrum (bottom) in medial view. Note the intraspecific asymmetry and the individual asymmetry of the anocleithrum. ano., anocleithrum; cl., cleithrum. Scale bar: 5 cm. 3D models are not to scale.

located at the mid-line, but this basal lamina cannot be observed in the imaging data.

In the fetus, the medial and lateral margins of the clavicle do not form a gutter and the clavicle does not totally surround the lateral angle of the scapulocoracoid (Fig. 6A). The posterior part of the clavicle is only in contact with the extracleithrum. There is no contact between the anterior twisted shanks of the right and the left clavicles. From pup 1 onwards, the clavicles are ventrally in contact and form a hemi-circle with the scapulocoracoid; the posterior part of the clavicle partially overlaps the cleithrum (Fig. 6B,C). In this stage, the lateral margin of the clavicle extends ventrally and begins to form a gutter. In pup 2 and the following stages, the lateral and medial margins of the clavicle form two small gutters that surround the lateral angle of the scapulocoracoid. From pup 2 onwards, the posterior tip of the clavicle overlaps the margins of both the cleithrum and extracleithrum.

- The scapulocoracoid (scc.)

This massive element is overlapped by the cleithrum, extracleithrum and clavicle (Figs 2 and 3). It is the only endochondral bone of the pectoral girdle. It is composed of two parts: a long triangular-shaped blade, with a dorsal tip and a ventral base, positioned on the internal side of the cleithrum, and a short and massive articular process for the pectoral fin, posteriorly oriented. The anterior margin of the triangular-shaped blade is concave. The lateral and dorsal angles of the scapulocoracoid are very sharp and respectively surrounded by the clavicle and the cleithrum (Fig. 2A). The massive articular process of the scapulocoracoid is posteriorly oriented along the body axis, and is round in transverse section. The end of this process is a flat quadrangular surface with a small articular head at the supero-lateral angle. This articular head corresponds to the glenoid process, forming a ball-and-socket joint (Miyake et al., 2016), and articulates with the first endoskeletal element of the fin.

In the fetus, the dorsal angle of the scapulocoracoid is rounded and slightly curved towards its outer side (Fig. 3). The dermal elements of the girdle do not lie directly on the triangular part of the scapulocoracoid but are separated by a large space (Fig. 6A). The articular process presents four concave faces in transverse section. From pup 1 onwards, the dorsal angle is straight and sharp. The dermal bones closely overlap the scapulocoracoid (Fig. 6). The articular process is more robust and large, and is rounded in transverse section (Fig. 3).

The pectoral fin

The pectoral fin of *Latimeria* is composed of different elements: mesomeres on the metapterygial axis, pre-axial elements (corresponding to the pre-axial radials and pre-axial accessory elements), and post-axial elements (corresponding to the post-axial accessory elements and the distal radial) (Fig. 7). According to Millot & Anthony (1958), the metapterygial axis of the fin consists of five axial

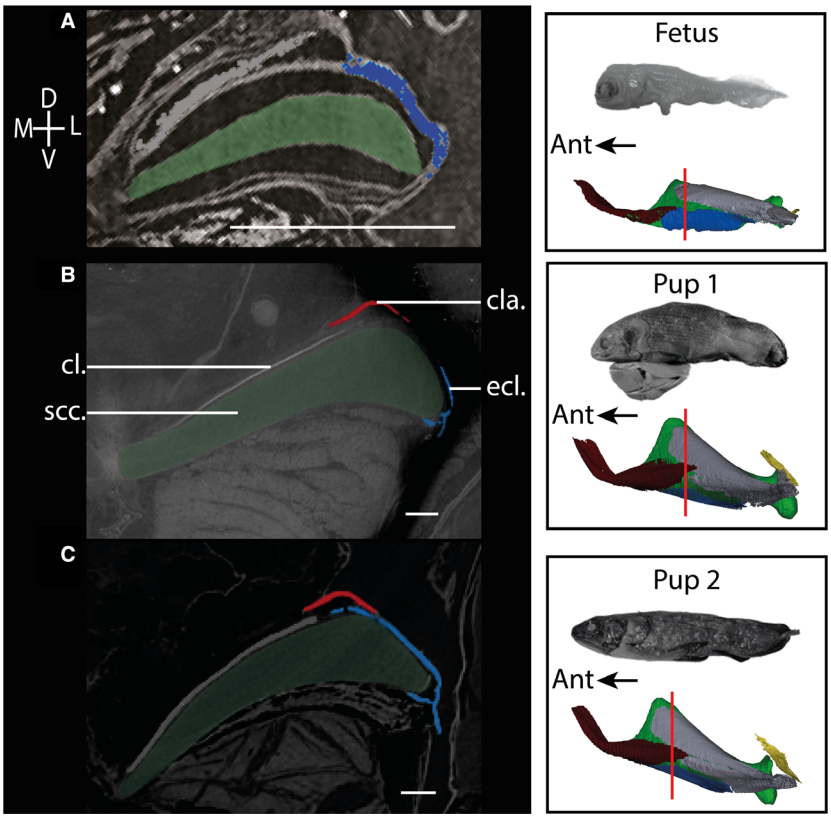

Fig. 6 *Latimeria chalumnae* – The fetus (A), the first (B) and second (C) pup. Left pectoral girdle in transverse section. The location of the transverse sections are shown by a red line on the dorsal view of the 3D models of the pectoral girdles. In the fetus, the anterior part of the clavicle is not well developed and partially overlaps the posterior part of the cleithrum (not visible in the transverse section). In the first pup, the anterior part of the clavicle partially overlaps the cleithrum, but not the extracleithrum, whereas from the second pup onwards the anterior part of the clavicle partially covers both the cleithrum and the extracleithrum. cl., cleithrum; cla., clavicle; ecl., extracleithrum; scc., scapulocoracoid. D, dorsal; L, lateral; V, ventral; M, medial. Specimens and 3D models are not to scale. Scale bar: 1 mm.

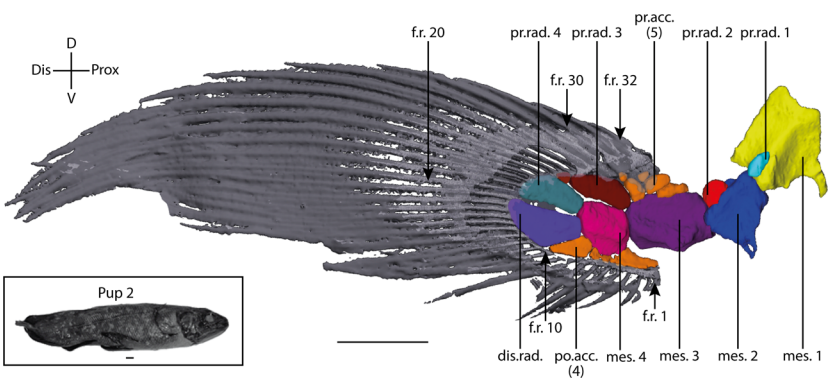

Fig. 7 *Latimeria chalumnae* – Second pup. Right pectoral fin in lateral view. f.r., fin ray; dis.rad., distal radial; mes., mesomere; po. acc., post-axial accessory elements; pr. acc., pre-axial accessory elements; pr. rad., pre-axial radial. Scale bar: 10 mm.

elements, named '*articles*' and numbered from proximal to distal. However, Ahlberg (1989) identified four mesomeres and one distal radial element. There are four pre-axial radial elements (Millot & Anthony, 1958; Forey, 1998) and a variable number of pre-axial and post-axial accessory elements (Millot & Anthony, 1958) (Fig. 7). The fin rays insert on the pre- and post-axial accessory elements, on the fourth pre-axial radial and on the distal radial (Fig. 7). According to Millot & Anthony (1958), the fifth axial element is different in shape from the first to fourth ones, and the fin rays articulate at its distal edge, whereas the previous axial elements do not articulate with the fin rays. In this regard, and following Forey (1998), we here refer to four mesomeres on the metapterygial axis and one distal radial that belongs to the post-axial elements. The term of 'mesomeres' is used after Jarvik (1980) for the subcylindrical radial segments of the principal axis in sarcopterygian fins.

According to Johanson et al. (2007), the three first axial elements are homologous to the humerus, ulna and ulnare of tetrapodomorphs and tetrapods. Similarly, the two first pre-axial radial elements are considered homologous to the radius and intermedium of tetrapods (Johanson et al., 2007). The reference position of the pectoral fin is with the fin positioned along the body, its leading edge oriented dorsally. This position corresponds to the

position of the pectoral fin of embryos within the oviduct (Forey, 1998).

1. The metapterygial axis

The first and second mesomeres (Forey, 1998) have a similar quadrangular prismatic shape with slightly concave faces, as described by Millot & Anthony (1958). The dorsal and ventral edges ('*bord supérieur*' and '*bord inférieur*' *cf*. Millot & Anthony, 1958) of the first mesomere form a ridge directed from the proximal to the distal side. The dorsal ridge is well developed and extends further than the distal end of the bone. The distal part of the ridge is directed to the medial plane ('*interne*' for Millot & Anthony, 1958), when the fin is in resting position. The ventral ridge is also well developed and has a hook ('*crochet*' for Millot & Anthony, 1958) directed towards the medial plane (Fig. 7, Supporting Information Fig. S1). The lateral and medial edges ('*externe*' and '*interne*' edges for Millot & Anthony, 1958) of the mesomeres are angular but smooth and do not form a ridge (Fig. S1).

Each mesomere is longer than wide and presents a proximal joint ('*extrémité antérieure*': Millot & Anthony, 1958) that is concave and a distal joint convex ('*extrémité postérieure*': Millot & Anthony, 1958).

- The first mesomere (mes. 1)

This mesomere has the same orientation in our virtual dissection as described by Millot & Anthony (1958) and we can define the four facets: the dorsomedial, the dorsolateral, the ventro-lateral and ventro-medial ('supéro-interne', 'supéro-externe', 'inféro-externe' and 'inféro-interne' of Millot & Anthony, 1958) (Fig. S1). It is the largest mesomere of the fin.

In the fetus, the transverse section of this mesomere shows four highly concave facets (Fig. 9A). The joint with the scapulocoracoid (called glenoid surface by Millot & Anthony, 1958) is also concave and is located on the lateral side of the mesomere, extending proximally (Figs 8 and 9C,D). The dorsal and ventral ridges of the first mesomere are slightly oblique to the medial plane at the distal end of the mesomere. These ridges begin at the level of the joint with the scapulocoracoid and end at the distal part of the first mesomere. From pup 1 onwards, the first mesomere is fully formed and presents a quadrangular prismatic shape. Its cross-section shows that its facets are less concave than in the fetus (Fig. 9B). The articular surface with the head of the scapulocoracoid is highly concave. As in the following stages, it is mainly located on the lateral side of the mesomere with only a lateral swollen margin (Fig. S1). From pup 1 to the adult, the morphology of the first mesomere does not change (except in size). In these stages, we can observe an asymmetry between the right and left sides. The left mesomere has a double hook that forms the beginning of a loop (Fig. 9E), whereas the right mesomere has only a single hook (Fig. 9F).

- The second mesomere (mes. 2)

This mesomere is smaller than the first one. As described by Millot & Anthony (1958), its proximal joint is less concave

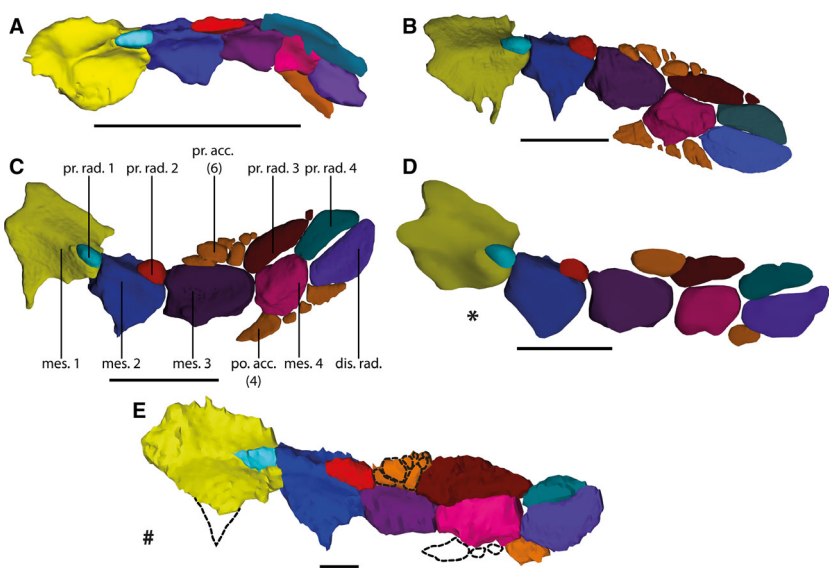

Fig. 8 *Latimeria chalumnae*. Pectoral fin of five different developmental stages in left lateral view (B–D) and right lateral view (mirrored, A,E). (A) The fetus. (B) The first pup. (C) The second pup. (D) The juvenile. (E) The adult. *The juvenile was scanned with MRI at low resolution, preventing the segmentation of the smallest elements. #The adult was scanned using a regular CT-scan and the resolution of the data did not allow the segmentation of some elements. Corresponding elements of the fin have been indicated in the same colour. The dotted line represents the pre-axial accessory elements, post-axial accessory elements and the hook on the mes. 1 of the stage 5 not segmented but known to exist based on prepared pectoral fins. dis.rad., distal radial; mes., mesomere; po. acc., post-axial accessory elements; pr. acc., pre-axial accessory elements; pr. rad., pre-axial radial. Scale bar: 2 mm (A), 10 mm (B–E).

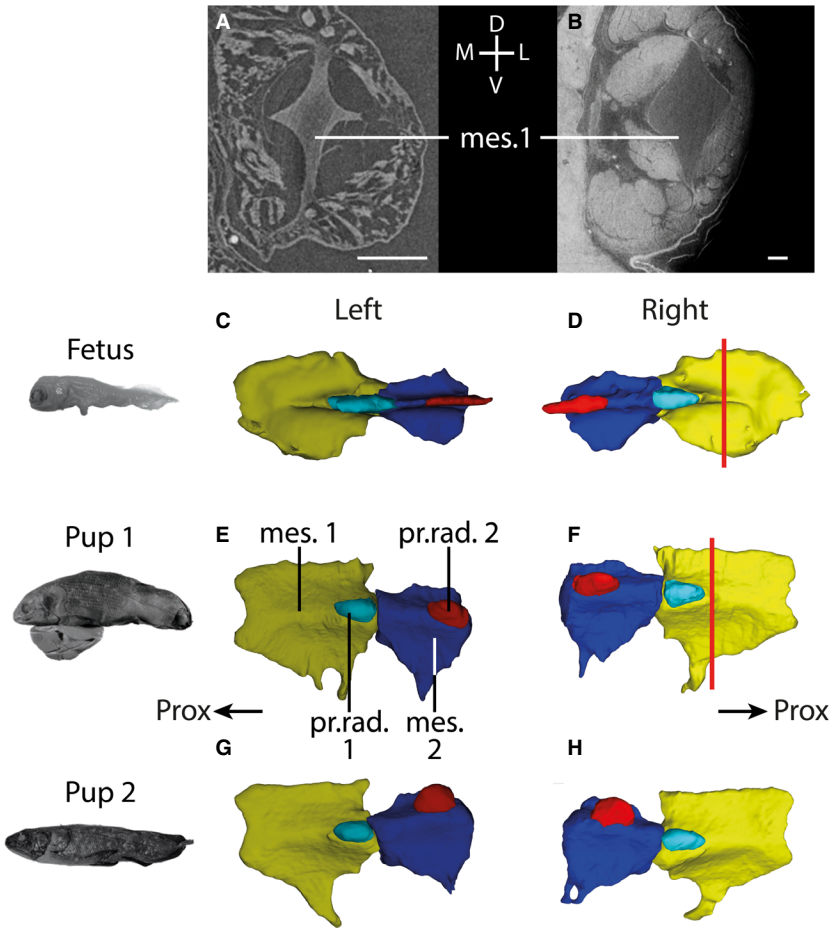

Fig. 9 *Latimeria chalumnae* – Stages 1–3. Transverse sections of the first mesomere in the fetus (A) and the first pup (B), and lateral views of the left (C,E,G) and right (D,F,H) proximal elements of the pectoral fin of the fetus (C,D), the first pup (E,F) and the second pup (G,H). The location of the transverse sections are shown in the 3D models of the corresponding mesomeres (red line). In the fetus, the mesomeres have strongly concave faces (A,C,D) compared with the following stages (B,E–H). Pre-axial radial elements 1 and 2 are proportionally longer than in the next stages, and extend more distally than the end of the corresponding mesomere (C,D). In the first (E,F) and second pup (G,H), the pre-axial radial elements are proportionally shorter and have an ovoid shape. The left first mesomere of the first pup (E) shows a double hook on the ventral ridge, whereas the right first mesomere of first pup (F) and the first mesomeres of the second pup show only a single hook (G,H). The right second mesomere of the second pup (H) has a loop-like hook on the ventro-lateral edge, whereas the left second mesomere (G) and the second mesomere of the first pup (E,F) show a single hook. mes., mesomere; pr. rad., pre-axial radial; D, dorsal; L, lateral; M, medial; V, ventral. Scale bar: 1 mm. 3D models are not to scale.

than that of the first mesomere. Despite a similar morphology to the first mesomere, its orientation is different and the bone shows a rotation around the fin axis (Fig. S1). The dorsolateral face of the mesomere 1 corresponds to the dorsal face of the mesomere 2, the ventrolateral face corresponds to the lateral face, the ventromedial face to the ventral face, and the dorsomedial face to the medial face (Fig. S1). The proximal joint of this mesomere is not in lateral position as in the first mesomere but covers the proximal surface (Fig. S1). This joint surface is less deep compared with the first mesomere and is surrounded by a peripheral swollen edge, whereas the first mesomere has only a lateral swollen edge around the proximal joint (Fig. S1). In the fetus, its morphology is similar to that of the first mesomere: longer than wide, thin, and with highly concave faces (Fig. 9C,D). In this stage, it is not clear whether there is a rotation of the elements along the metapterygial axis. From pup 1 onwards, it is fully formed with a quadrangular prismatic shape and concave faces. As for the first mesomere, the second mesomere shows some asymmetry. In pup 2, the ventrolateral ridge of the right fin has a double hook that forms a loop (Fig. 9G), whereas on the left fin, the second mesomere only has a single hook (Figs 8 and 9H).

- The third mesomere (mes. 3)

As for the second mesomere, this element shows a rotation around the axis of the fin. Here, the dorsal face of the second mesomere corresponds to the dorsomedial face, the lateral face to the dorsolateral face, the ventral face to the ventrolateral face, and the medial face to the ventromedial face. Therefore, the dorsal edge of the first mesomere corresponds to the medial edge of this mesomere and the dorsolateral face of the first mesomere to the dorsomedial face. This mesomere is more transversely flattened than the previous one. The dorsal and ventral ridges of the first mesomere correspond to the medial and lateral ridges. As for the previous mesomere, the ridges are on the medial and lateral edges of the third mesomere (corresponding to the dorsal and ventral edges of the first mesomere), separating the dorsomedial and ventromedial faces (and dorsolateral and ventrolateral faces) of the mesomere. These two ridges, directed from proximal to distal, present the same shape. The proximal first third is oblique and slopes down to the ventral side. The distal two-thirds slope slightly up until the distal extremity of the mesomere (Fig. 10C–F). The lateral ridge does not present a hook, unlike the ventral ridge of the first mesomere and the ventro-lateral ridge of

the second mesomere. The concave proximal joint is less deep than that of the previous mesomere. The distal end of this mesomere is highly convex and articulates with the fourth mesomere and the third pre-axial radial. In the fetus, its morphology is similar to previous mesomeres. From pup 1 onwards, it is fully formed, and its morphology does not change until the adult stage (Figs 8 and 10).

- The fourth mesomere (mes. 4)

This is the smallest mesomere of the fin. It has the same orientation as the third mesomere and it has the same transverse flattening. Its ventral edge forms a large ridge, whereas its dorsal edge is flat (Figs 7 and 10). The lateral and medial edges of the fourth mesomere form a large bulge and there is a small oblique ridge on the proximal part of the medial edge. This mesomere is surrounded by the third pre-axial radial element at its dorsal edge and by the post-axial accessory elements at its ventral edge (Figs 7 and 10). In the fetus, as for the previous elements, the fourth mesomere is thin, with highly concave faces in transverse cross-section. The ventral edge shows a small ridge, smaller than in the next stages (Fig. 10A,B). The dorsal edge of the fourth mesomere forms a massive ridge. The lateral and medial edges of the mesomere each form a thin ridge directed from proximal to distal. The medial thin ridge follows the proximo-distal mid-line along the medial face of mesomere and the lateral ridge is located more ventrally on the fourth mesomere. From pup 1 onwards, it is fully formed and its morphology does not change until the adult stage (Figs 8 and 10C–F). The dorsal edge no longer has its triangular shape and becomes flat. The lateral and medial ridges of the fetus now form a bulge directed from proximal to distal and it is more difficult to distinguish the dorsolateral and ventrolateral faces on the lateral side of the mesomere (and the dorsomedial and ventromedial faces from the medial side of the mesomere) (Fig. 10C–F).

2. The pre-axial elements

The pre-axial radial elements are located on the dorsal side of the fin (corresponding to the pre-axial side of the fin/limb of most sarcopterygians; Forey, 1998), near to the joint between the mesomeres of the fin. The first and second pre-axial radials have a different morphology from the third and fourth pre-axial radials (Millot & Anthony, 1958). The two first pre-axial radials have an egg-like shape, whereas the others are thin and elongated.

- The first pre-axial radial (pr. rad. 1)

This is positioned at the distal part of the lateral edge of the first mesomere (pre-axial edge), near the joint with the second mesomere. It is slightly shifted towards the dorsolateral face of the first mesomere (Figs 7–9). It is egg-shaped and slightly thinner on the proximal side. In the fetus, this radial extends to the proximal part of the second mesomere and the distal part of the first mesomere (Fig. 9C,D), but from pup 1 onwards, it only covers the first mesomere (Fig. 9E–H). The right and left first pre-axial radials present a different shape. Whereas the right element already shows its ovoid shape, the left element is thinner in transverse section and elongated, and extends more broadly to the second mesomere.

- The second pre-axial radial (pr. rad. 2)

This radial covers the distal part of the dorsolateral edge of the second mesomere, near the joint with the third mesomere. As for the first pre-axial radial, it is slightly shifted towards the dorsal face of the second mesomere and is egg-shaped (Figs 7–9). According to Millot & Anthony (1958), this element is thinner and more elongated than the first pre-axial radial. However, our segmentation and the different isolated pectoral fins of adult specimens (CCC 6; CCC 7; CCC 14; CCC 19) show a similar size and shape of the two elements. In the fetus, this second pre-axial radial is elongated and thin in transverse section and covers the proximal part of the third mesomere (Figs 8 and 9C,D). From pup 1 onwards, the second pre-axial radial is less elongated and egg-shaped, and covers only the distal part of the second mesomere (Figs 8 and 9E–H).

- The third pre-axial radial (pr. rad. 3)

This radial differs from the previous radials in shape; it is thin and elongated, oval-shaped, and taller than the fourth mesomere that it covers (Fig. 7). At its distal end, there is a small pointed element, which is the tip of the third pre-axial radial. This element carries fin rays 25–28 (Fig. 7). The proximal part of this element is straight and it articulates with the third mesomere. In the fetus, it could only be segmented for the right fin. This element is closely associated with the fourth pre-axial radial and the pre-axial accessory elements and is part of a large cartilaginous plate (Fig. 10A, B). In pup 1, the cartilaginous plate is segmented and the third pre-axial radial is differentiated from the fourth pre-axial radial and the pre-axial accessory elements (Fig. 10). From pup 1 onwards, the third pre-axial radial presents its elongated oval shape and has a small separated tip.

- The fourth pre-axial radial (pr. rad. 4)

This element is positioned at the distal end of the fin endoskeleton in association with the distal radial. As for the third pre-axial radial, this element is elongated and thin, but it has a trapezoidal shape with three straight edges and one curved edge (Figs 7 and 10). The ventral straight edge is in contact with the distal radial and its dorsal edge is in contact with the third pre-axial radial and its tip. It articulates with distal part of the fourth mesomere next to its proximal straight edge (Fig. 10). Its distal edge is curved and carries fin rays 20–24 (Fig. 7). In the fetus, it appears that the third pre-axial radial and the fourth pre-axial radial form a unique cartilaginous plate that covers at least the fourth mesomere and the distal radial in the left fin

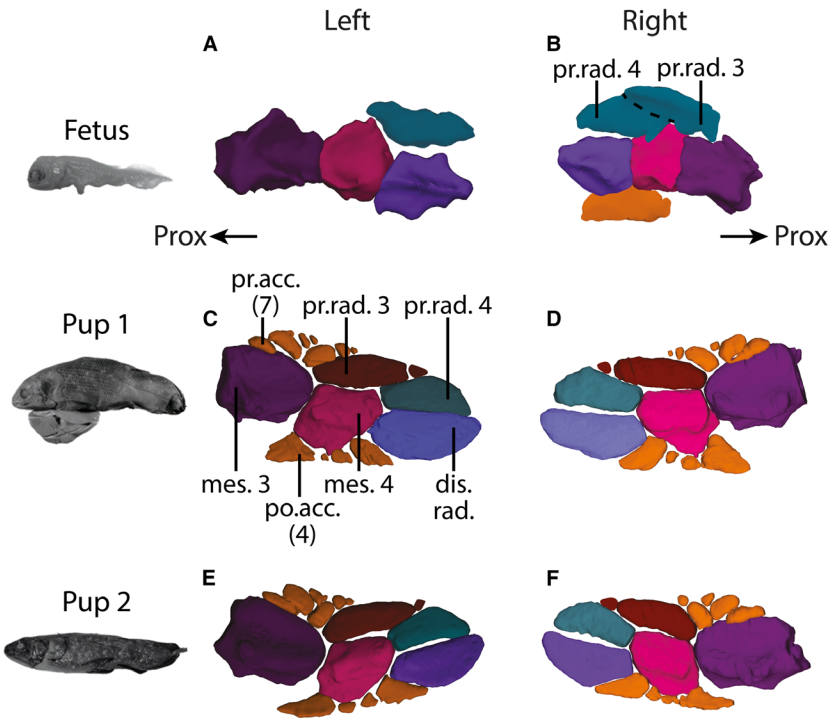

Fig. 10 *Latimeria chalumnae* – Stages 1–3. Distal part of the left (A,C,E) and right (B,D,F) pectoral fins of the fetus (A,B), the pup 1 (C, D) and the pup 2 (E,F) in lateral views. In the fetus, the right pectoral fin shows a large cartilaginous plate (blue) that corresponds to pre-axial radials 3 and 4 and the pre-axial accessory elements in the following stages. The first and second pups show variation and asymmetry in the number of pre-axial accessory elements. dis.rad, distal radial; mes., mesomere; po. acc., post-axial accessory elements; pr. acc., pre-axial accessory elements; pr. rad., pre-axial radial. Not to scale.

(Fig. 10A) as well as the third mesomere in the right fin (Fig. 10B). Between the fetus stage and the pup 1 stage, this element becomes segmented into several elements: the third pre-axial radial with its pre-axial accessory elements and its tip, and the fourth pre-axial radial described just above (Figs 8 and 10). From pup 1 onwards, the fourth pre-axial radial presents its trapezoidal shape (Fig. 10C–F).

• Pre-axial accessory elements (pr. acc.)

These elements (called 'éléments accessoires de la troisième pièce radiale préaxiale' by Millot & Anthony, 1958) are positioned at the dorsal edge of the third mesomere and are associated to the third pre-axial radial. There is one large element in contact with the third mesomere, one large element in contact with both the third mesomere and the previous element that carries fin rays 31 and 32, and one large element in contact with the third mesomere and the third pre-axial radial, which carries fin rays 29 and 30 (Fig. 7). There are also several smaller elements, between two and four, in contact with the larger elements or with the third pre-axial radial; their number varies depending on the development stage (Figs 7, 8 and 10). In the fetus, there are no differentiated pre-axial accessory elements. These elements belong to the same large cartilaginous plate as the third pre-axial radial and the fourth pre-axial radial (Fig. 10A,B). From pup 1 onwards, the cartilaginous plate becomes segmented in several elements and the pre-axial accessory elements are differentiated from the third pre-axial radial and the fourth pre-axial radial (Fig. 10). It seems that the number of pre-axial accessory elements is not fixed and can differ between the right and left fins within an individual (Fig. 7). In pup 1, there are six elements on the right fin with three small elements, and seven elements on the left fin with four small elements. In pup 2, there is the same organization, with three small pre-axial accessory elements of the right fin but only two small elements on the left fin (associated with the three large elements). In the adult, Millot & Anthony (1958) described seven elements on the pre-axial accessory elements, three large elements and four small elements. Our 3D segmentation shows only one large cartilaginous element identified by μCT, but the different isolated pectoral fin skeletons show seven elements, as described by Millot & Anthony (1958).

3. The post-axial elements

• The distal radial (dis. rad.) (Fig. 7)

As described by Millot & Anthony (1958), this element is transversely flattened and has an elongated trapezoid shape. Its shape is similar to the fourth pre-axial radial and it is symmetric, but slightly taller (Figs 7 and 10). It has three straight edges and one curved convex edge. In transverse section the distal radial present two slightly convex faces (Supporting Information Fig. S2). Its dorsal straight edge is aligned with the proximo-distal axis of the fourth mesomere and it is close to the fourth pre-axial radial element. The proximal joint is straight. Its ventral edge is straight and in contact with the distal post-axial accessory element. The curved edge is positioned at the distal part of the ventral edge of this element. It is on this edge that fin rays 11–19 are inserted (Fig. 7). In the fetus, the distal radial already presents a shape similar to that observed in the

adult. It is transversely flattened, but presents a lateral ridge directed from proximal to distal (Fig. 10A,B). In pup 1, there is no lateral ridge on this element (Fig. 10C,D). From pup 2 onwards, there is a small swelling on its dorsal edge. This swelling is triangular-shaped, as wide as its edge on the proximal part, then decreasing in size (Fig. 10E,F).

- The post-axial accessory elements (po. acc.)

According to Millot & Anthony (1958), there are five post-axial accessory elements in the adult stage. However, in the different isolated pectoral fins of adult specimens observed (CCC 6, CCC 7, CCC 14 and CCC 19) we can see only four elements, aligned along the ventral ridge of the fourth mesomere. The proximal and the distal post-axial accessory elements are the largest ones and have a similar shape. The proximal element articulates with the proximal part of the ventral edge of the fourth mesomere. It is triangular-shaped with the tip directed to the proximal side of the fin and leaves a large gap between this element and the third mesomere (Figs 7, 8 and 10). The second and third post-axial accessory elements are small and globular. The distal element is similar to the first element. This element is in contact with the distal part of the ventral edge of the fourth mesomere and the ventral edge of the distal radial. The first 10 fin rays insert on the ventral edge of these post-axial accessory elements: rays 1–5 on the first element, ray 6 on the second element, ray 7 on the third, and rays 8–10 on the fourth element (Fig. 7). In the fetus, only one large post-axial accessory element was identified in the μCT (Fig. 10B). This element is in contact with the fourth mesomere and the proximal part of the ventral edge of the distal radial. It appears segmented in pups 1 and 2, similar to the pre-axial cartilaginous plate. In pup 1, we can observe an asymmetry between the right and left fin for these elements. In the right fin, the elements are as described above, but in the left fin, the third element is slightly different, being flat and trapezoidal-shaped (Fig. 10C). In pup 2, there is no asymmetry between the right and left pectoral fins for these elements. In the juvenile and adult, the μCT data do not allow us to identify more than one small element (Fig. 8).

4. The fin rays

There are 32 fin rays on the pectoral fin. There are numbered 1 to 32 from the ventral side to the dorsal side (Fig. 7). As described by Millot & Anthony (1958), the proximal part of the fin ray is bifurcated, one branch inserting on the lateral side of the fin and the other on the medial side. The first ray is very small, the following are longer, increasing in length until ray 20, after which the length of the fin rays decreases. The fin rays of the pre-axial side of the fin insert largely on the pre-axial radials elements: rays 29–32 insert on the pre-axial accessory elements, rays 25–28 on the third pre-axial radial, and rays 20–24 on the curved edge of the fourth pre-axial radial. On the post-axial side of the fin, the fin rays insert only on the edge of the elements: fin rays 11–19 on the curved edge of the distal radial and fin rays 1–10 on the edge of the post-axial accessory elements. In the fetus, the fin web is rounded and there seems to be no clear leading edge. From pup 1 onwards, the fin web has the same morphology as in the adult, forming a fin web that is elongated and pointed, with a convex leading edge and a concave trailing edge.

Discussion

As the period of gestation remains unknown in extant coelacanths, it was consequently not possible to establish precise relationships between the known ontogenetic stages in vertebrates and those described here for *Latimeria*. We have gathered five clearly different ontogenetic stages: three prenatal stages, one juvenile stage and one adult stage.

The pectoral girdle

The pectoral girdle shows different arrangements within the different vertebrate groups, with various types of relationships between the dermal and endoskeletal elements in terms of the mode of locomotion (McGonnell, 2001). The dermal anocleithrum (in sarcopterygians) or postcleithrum (in actinopterygians), cleithrum and clavicle are primitively present in all osteichthyans (Gosline, 1977; Friedman & Brazeau, 2010; Zhu et al., 2012a). The majority of osteichthyans also have a supracleithrum and/or a post-temporal element, both small elements located in the most dorsal part of the girdle as in early tetrapodomorphs (Coates & Ruta, 2007; Friedman & Brazeau, 2010). Coelacanths have the anocleithrum, cleithrum and clavicle in common with the other osteichthyans, but also a supernumerary dermal bone, the extracleithrum, which is considered as a synapomorphy of the group (Forey, 1998). The endoskeletal element of the pectoral girdle, the scapulocoracoid, is present in all vertebrates and is covered by the cleithrum and clavicle in osteichthyans (McGonnell, 2001). In osteichthyan fishes, the scapulocoracoid is usually small compared with other elements of the pectoral girdle, and the cleithrum forms a large part of the girdle (Janvier, 1996; McGonnell, 2001; Zhu & Schultze, 2001). However, in *Latimeria chalumnae* the scapulocoracoid is proportionally massive (Figs 3 and 5) and is, as the cleithrum, the largest element of the girdle. A large scapulocoracoid is also present in the lungfish *Neoceratodus forsteri* (Rosen et al., 1981; Johanson et al., 2004) and is considered convergent with coelacanths by Coates & Ruta (2007). Within tetrapodomorphs, there is an evolutionary trend towards a reduction of the dermal part of the girdle (clavicle, cleithrum), whereas the endochondral scapulocoracoid becomes the main component of the girdle in tetrapods (McGonnell, 2001; Vickaryous & Hall, 2006). The presence of a large scapulocoracoid or scapula + coracoid in

tetrapods and in the coelacanth *Latimeria* is also considered convergent. Indeed, early tetrapodomorphs such as *Eusthenopteron* (Andrews & Westoll, 1970) have proportionally small scapulocoracoids, similar to extinct coelacanths as observed in the Triassic coelacanth *Laugia groenlandica* (Stensiö, 1932; Millot & Anthony, 1958) and the Devonian coelacanth *Diplocercides* (Stensiö, 1922). However, it is necessary to be careful with this assumption. Indeed, unlike the dermal elements of the girdle, the coelacanth scapulocoracoid is largely cartilaginous and it is consequently possible that only the most ossified part of this element has been preserved in fossils (Forey, 1998). According to Forey (1981), the scapulocoracoid of the Carboniferous coelacanth *Rhabdoderma* was probably more substantial than the preserved mineralized portion, and fits into the groove present in the internal face of the cleithrum as observed in *Latimeria*. If this assumption is correct, the presence of the groove on the internal side of dermal bones of the girdle in fossil coelacanths, as in *Diplurus* (Schaeffer, 1952), *Rhabdoderma* (Forey, 1981) and *Trachymetopon* (Dutel et al., 2015), delimits the lateral expansion of the scapulocoracoid.

In most osteichthyans the pectoral girdle is formed early in development before the fins or limbs. The cleithrum and clavicle are dermal bones and are known to be the first to appear, the scapulocoracoid appearing later in the development of actinopterygians (Jollie, 1980; Faustino & Power, 1999; Koumoundouros et al., 2001) and of the lungfish *Neoceratodus* (Johanson et al., 2004; Joss & Johanson, 2007). In *Latimeria chalumnae*, our observations suggest a similar development, as all the elements of the pectoral girdle are present in the fetus. However, the scapulocoracoid seems deflated and is not in tight contact with the dermal bones (Figs 3 and 6). Later in development, an expected radially outward growth of the scapulocoracoid leads to the close overlapping of the scapulocoracoid by the cleithrum, the extracleithrum and the clavicle, as observed from pup 1 onwards (Fig. 6). These observations allow us to assume that the scapulocoracoid is formed later in development than are the dermal bones in *Latimeria* as in most vertebrates. The scapulocoracoid consists of a single massive element (Millot & Anthony, 1958) in the early development of the pectoral girdle. This development of the scapulocoracoid of *Latimeria* agrees with Schaeffer's (1941) observation of a complete co-ossification of the scapular and coracoid elements of the girdle for *Undina* and *Macropoma*. However, the development of the endoskeletal bone of the pectoral girdle is different from the actinopterygians. Indeed, in actinopterygians (except for acipenseriforms: Jollie, 1980; Davis et al., 2004), there are two regions of ossification inside the cartilaginous scapulocoracoid plate that correspond to the scapular and coracoid regions of the girdle (Patterson, 1982; Cubbage & Mabee, 1996; Grandel & Schulte-Merker, 1998). In *Neoceratodus*, as for *Latimeria*, there are no distinct ossification centres for the scapular and coracoid regions inside the scapulocoracoid. However, unlike the coelacanth, these two regions are distinct in the adult lungfish and are not co-ossified (Johanson et al., 2004).

The anocleithrum is the element of the girdle that proportionally grows the most during development despite remaining the smallest bone of the girdle at the adult stage (Fig. 3). The small and rod-like anocleithrum in *Latimeria* is different in size and proportion from the anocleithra known in other sarcopterygian fishes such as *Neoceratodus* and tetrapodomorph fishes (Coates & Ruta, 2007). The anocleithrum of *Latimeria* provides an insertion for the large *levator externus 5* muscle of the branchial arches musculature (Millot & Anthony, 1958; Forey, 1998; Carvalho et al., 2013), likely similar to *Neoceratodus* (Carvalho et al., 2013). However, the homology between the anocleithrum bones of different sarcopterygians has been challenged (Campbell et al., 2006) and remains to be validated.

In the early stages of development there is a reorientation of the pectoral girdle inside the body. The reorientation of bones during development has been shown in several groups of vertebrates. It is well documented for the pelvic girdle in lissamphibians (Rocková & Rocek, 2005; Pomikal et al., 2011; Manzano et al., 2013), chicken (Nowlan & Sharpe, 2014) and mice (Pomikal & Streicher, 2010), and for the pectoral girdle in chelonians (Nagashima et al., 2007). However, the mechanisms of rotation and reorientation of the girdles remain largely unknown. As for the reorientation of the digits during the development in some birds (Botelho et al., 2014), the reorientation of the pectoral girdle in *Latimeria* is probably tightly linked to its interactions with the development of the adjacent muscles.

The pectoral fin

The endoskeletal elements of the pectoral fin known in the adult stage are already present in the fetus, except for the pre-axial accessory elements and pre-axial radial elements 3 and 4. The axial elements of the pectoral fin, like the scapulocoracoid, seem deflated in the fetus, and their development between the fetus and pup 1 suggests a significant process of radially outward growth (Fig. 8). The large distal cartilaginous plate in the fetus corresponds to the most distal radial elements (pre-axial radials 3 and 4, pre-axial accessory elements) in pup 1. The post-axial accessory elements show a similar development, with the post-axial cartilaginous plate in the fetus corresponding to four post-axial accessory elements in pup 1 (Fig. 8). Millot & Anthony (1958) already proposed the fragmentation of a unique cartilaginous plate to form the radial elements. Observations made on the earliest stage confirm the presence of non-differentiated large plates and support this hypothesis. Moreover, in the fetus, the cartilaginous plate articulates with the third and fourth mesomeres and the distal radial, suggesting a positional homology to the pre-axial accessory elements and the pre-axial radials 3 and 4, as these

elements are respectively articulated with the third and fourth mesomeres and the distal radial in the later stages of development (Figs 8 and 10).

This splitting of a single endochondral plate to form the elements of the fin is also known in some other groups of vertebrates. This mechanism has been observed in actinopterygians such as *Polyodon* (Davis et al., 2004; Mabee & Noordsy, 2004), zebrafish *Danio rerio*, bichir *Polypterus senegalus* (Grandel & Schulte-Merker, 1998) and sturgeon *Acipenser* (Davis et al., 2004). The splitting of the endoskeleton of the fin is accomplished by a decomposition of the extracellular matrix of the endoskeletal plate, leading to the formation of the proximal radials (pro- and mesopterygium) (Davis et al., 2004; Nakamura et al., 2016). The primitive condition of the pectoral fin of sarcopterygians is thought to be polybasal with pro-, meso- and metapterygium, as in actinopterygians (Zhu & Yu, 2009). However, crown sarcopterygians, including coelacanths, have lost their pro- and mesopterygium and only retain the metapterygium leading to the monobasal condition of the fin (Rosen et al., 1981; Janvier, 1996; Zhu & Yu, 2009). In the acipenseriforms *Acipenser* and *Polyodon*, the metapterygial elements are formed outside the endoskeletal plate as an extension of the scapulocoracoid (Davis et al., 2004; Mabee & Noordsy, 2004). These elements are formed in a similar way to the distal radials of the fins of non-tetrapod sarcopterygians and the limbs in tetrapods (Davis et al., 2004), with a condensation of the mesenchyme from proximal to distal (Shubin & Alberch, 1986; Joss & Longhurst, 2001).

The development of the metapterygial axis in *Latimeria* might result from a process of segmentation known in other sarcopterygians and in *Polyodon*. However, this process occurs in the earliest stages of the development of the fin or limb, and only for the formation of the different cartilaginous elements of the endoskeletal axis before the ossification of these elements (Shubin & Alberch, 1986; Joss & Longhurst, 2001; Cohn et al., 2002). Due to the reduced ontogenetic series used in this study, we cannot confirm a segmentation process, as the elements are already formed and only growth of the separated endoskeletal elements can be observed. For coelacanths, it is then not possible to identify the mechanism involved in the formation of the metapterygial axis or in the splitting of the cartilaginous plate into pre-axial radial elements or post-axial accessory elements. However, the splitting of the two pre-axial and post-axial cartilaginous plates to form, respectively, the third and fourth pre-axial radials and the pre-axial accessory elements, and the post-axial accessory elements, seems to be different from the decomposition process of the extracellular matrix of the endoskeletal disc to form the radial elements, as known in actinopterygians. Indeed, in actinopterygians, it is the precartilaginous plate that splits during development and forms the different radial elements. However, this splitting occurs before the condensation of the precartilaginous plate (Grandel & Schulte-Merker, 1998; Davis et al., 2004). In *Latimeria*, it appears that the cartilaginous plate is already condensed in the fetus. This is clearly visible from the μCT data and the different elements of the fins have the same contrast as that of other endochondral bones of the body.

Evolution of the pectoral fin morphology in coelacanths and tetrapodomorph fishes

The radial elements of the pectoral fin are asymmetrically organized around the metapterygial axis. Indeed, each mesomere of the fin is associated with a pre-axial element (radial and/or accessory), whereas only the fourth mesomere is associated with radial elements on its post-axial region (distal radial and accessory elements; Fig. 7). However, the general shape of the first and second pre-axial radials, small and rounded, is clearly different from that of the more distal radials, which are longer and flattened (Fig. 7), as previously reported (Millot & Anthony, 1958). This difference in shape between the pre-axial radial elements gives a lobe-shaped morphology to the pectoral fin of *Latimeria* compared with the fan-shaped fin morphology known in tetrapodomorph fishes. By contrast, the dermal fin rays are arranged almost symmetrically around the main axis of the pectoral fin and they do not insert on the pre-axial radials 1 and 2 (Fig. 7). The asymmetrical condition of the pectoral fin is more pronounced in the early stage of development. In the fetus, the first and second pre-axial radials, extending on the next mesomere, are proportionally longer than in the following stages (Figs 8 and 9C,D), where these elements are small and only associated with one mesomere (Figs 7, 8 and 10E–H). The proportional reduction of the size of the proximal pre-axial radials with respect to the rest of endochondral elements gives the fin a more lobe-shaped aspect. Developmental data seem to corroborate the scenario of an evolution of the pectoral fin towards a lobe-shaped morphology based on rare fossil coelacanth specimens. Indeed, the species *Shoshonia arcopteryx* (Friedman et al., 2007) from the Devonian of the USA, has elongated and flattened radials on the pre-axial side of the fin. The most proximal pre-axial radials are elongated in *Shoshonia* and are different from the short and rounded first and second pre-axial radials in adult *Latimeria*, providing the fin with a more fan-shaped morphology. Interestingly, the earliest stage of *Latimeria* also presents elongated proximal pre-axial radials. As seen in *Latimeria* from the fetus stage, only the distal mesomere is associated with a post-axial radial. The fin rays of *Shoshonia* are associated with all the pre-axial radials, which gives the fin a more asymmetrical profile of the fin web (Friedman et al., 2007). This asymmetrical disposition of the fin rays is also observed in other fossil coelacanths (Forey, 1998; Friedman et al., 2007), including *Laugia groenlandica* (Stensiö, 1932) from the Triassic of Greenland. The condition observed in these fossils is thus

different from the near-symmetrical arrangement of the fin rays in *Latimeria*. An asymmetrical arrangement of the radial elements and fin rays along the metapterygial axis is also observed in tetrapodomorph fishes (Andrews & Westoll, 1970; Shubin et al., 2006; Friedman et al., 2007), whereas in dipnomorph fishes the pectoral fin is very symmetrical (Ahlberg, 1989; Friedman et al., 2007). The fin rays usually insert on the pre- and post-axial radial elements, except in osteolepiforms, where they also insert on the post-axial process of the mesomeres (Friedman et al., 2007). According to several authors it is possible that the post-axial process and the post-axial radials have a same ontogenetic origin, which could explain the insertion of the fin rays on the mesomere (Jarvik, 1980; Friedman et al., 2007).

In contrast, the endochondral elements in the pectoral fin of dipnomorphs are almost symmetrical, with an arrangement of pre-axial and post-axial radials all along the metapterygial axis (Ahlberg, 1989; Friedman et al., 2007; Jude et al., 2014). However, the condition observed in lungfish appears to be highly derived with respect to ancestral sarcopterygians. The presence of an internally and externally asymmetrical pectoral fin in coelacanths and other lobe-finned fishes suggests that this condition is ancestral for sarcopterygians, as first proposed by Ahlberg (1989). This interpretation is supported by our observations made on the development of *Latimeria*. The particular morphology of the pectoral fin in *Latimeria* might be linked to changes in the mobility of the fin and in the locomotion, but this hypothesis remains to be tested.

Conclusion

The bony elements of the girdle and pectoral fin of the extant coelacanth *Latimeria* are nearly fully developed in the earliest stage of the ontogenetic series described here. During the first steps of pectoral fin development, there is a reorientation of the girdle putting the scapulocoracoids and the clavicles in the ventro-medial region of the two girdles in contact. The anocleithrum is the dermal bone of the girdle that proportionally grows the most during the development, further showing considerable morphological plasticity. The scapulocoracoid is robust, which is unusual in most osteichthyans with the exception of tetrapods. The earliest developmental stage specimen shows a deflated scapulocoracoid and a lack of contact between the mesomeres and the scapulocoracoid with the dermal bones of the girdle. This early stage specimen also presents two large cartilaginous plates, on the pre-axial and post-axial sides of the fin that later split into the pre-axial accessory elements and the third and fourth pre-axial radials, and in the post-axial accessory elements. The internal shape of the pectoral fin further becomes progressively more lobe-shaped due to a proportional reduction of the proximal pre-axial radials during development. Our developmental data corroborate previous fossil evidences and reinforce the hypothesis that the lobe-shaped pectoral fin in the living coelacanth derives from the primitive fan-shaped condition of sarcopterygians.

Acknowledgements

We thank R. Bills and A. Paterson (South African Institute for Aquatic Biodiversity, SAIAB) and D. Neumann (Zoologische Staatssammlung München, ZSM) for the loan of the fetus and pup 2 specimens, respectively. We are grateful to the European Synchrotron Radiation Facility (ESRF, Grenoble, France) for granting beam time and providing assistance in using beamline ID19 (Proposal EC-1023), and M. Garcia at AST-RX, plate-forme d'accès scientifique à la tomographie à rayons X (UMS 2700, MNHN, Paris, France) for the X-ray tomography scans. We thank F. Goussard (UMR 7207 CR2P MNHN-CNRS-Sorbonne Université, Paris, France) for his assistance in the 3D imaging work. We thank C. Bens and A. Verguin of the Collections de Pièces anatomiques en Fluides of the MNHN de Paris. We thank B. Lindow (Natural History Museum of Denmark) for the loan of fossils of Laugia groenlandica. This work was supported by a grant from Agence Nationale de la Recherche in the LabEx ANR-10-LABX-0003-BCDiv, program 'Investissements d'avenir' no ANR-11-IDEX-0004-02.

Author contributions

R.M., G.C. and M.H. designed the project. H.D. and P.T. performed the synchrotron scans. M.D.S. produced the magnetic resonance imaging acquisitions. H.D., G.C. and M.H. produced the conventional microtomographic acquisitions with the assistance of local staff. R.M. segmented the scans and did the 3D rendering of all developmental stages. R.M., G.C., A.H. and M.H. interpreted the results. R.M. wrote the manuscript. G.C., A.H, H.D., P.T. and M.H. revised the manuscript.

Data availability statement

All the data are available by request from the authors.

References

Ahlberg PE (1989) Paired fin skeletons and relationships of the fossil group Porolepiformes (Osteichthyes: Sarcopterygii). *Zool J Linn Soc* **96**, 119–166.

Ahlberg PE (1991) A re-examination of sarcopterygian interrelationships, with special reference to the Porolepiformes. *Zool J Linn Soc* **103**, 241–287.

Amaral DB, Schneider I (2017) Fins into limbs: Recent insights from sarcopterygian fish. *Genesis* **56**, 1–8.

Amemiya CT, Alfoldi J, Lee AP, et al. (2013) The African coelacanth genome provides insights into tetrapod evolution. *Nature* **496**, 311–316.

Andrews SM, Westoll TS (1970) The postcranial skeleton of *Eusthenopteron foordi* Whiteaves. *Earth Environ Sci Trans R Soc Edinburgh* **68**, 207–329.

Anthony J (1980) Evocation des travaux français sur *Latimeria* notamment depuis 1972. *Proc R Soc B Biol Sci* **208**, 349–367.

Botelho JF, Smith-Paredes D, Nuñez-Leon D, et al. (2014) The developmental origin of zygodactyl feet and its possible loss in the evolution of Passeriformes. *Proc R Soc B Biol Sci* **281**, 20140765.

Campbell KSW, Barwick RE, den Blaauwen JL (2006) Structure and function of the shoulder girdle in dipnoans: new material from *Dipterus valenciennesi*. *Senckenb Lethaea* **86**, 77–91.

Carvalho M, Bockmann FA, de Carvalho MR (2013) Homology of the fifth epibranchial and accessory elements of the ceratobranchials among gnathostomes: insights from the development of ostariophysans. *PLoS ONE* **8**, e62389.

Casane D, Laurenti P (2013) Why coelacanths are not 'living fossils': A review of molecular and morphological data. *BioEssays* **35**, 332–338.

Cavin L, Guinot G (2014) Coelacanths as 'almost living fossils'. *Front Ecol Evol* **2**, 1–5.

Cavin L, Mennecart B, Obrist C, et al. (2017) Heterochronic evolution explains novel body shape in a Triassic coelacanth from Switzerland. *Sci Rep* **7**, 1–7.

Clack JA (2009) The fin to limb transition: new data, interpretations, and hypotheses from paleontology and developmental biology. *Ann Rev Earth Planet Sci* **37**, 163–179.

Clack JA (2012) *Gaining Ground: The Origin an Evolution of Tetrapods*. Bloomington: Indiana University Press.

Coates MI (2003) The evolution of paired fins. *Theory Biosci* **122**, 266–287.

Coates MI, Ruta M (2007) Skeletal changes in the transition from fins to limbs. In: *Fins into Limbs – Evolution, Development, and Transformation*. (ed. Hall BK), pp. 15–38. Chicago: The University of Chicago Press.

Coates MI, Jeffery JE, Ruta M (2002) Fins to limbs: What the fossils say. *Evol Dev* **4**, 390–401.

Cohn MJ, Lovejoy CO, Wolpert L, et al. (2002) Branching, segmentation and the metapterygial axis: Pattern versus process in the vertebrate limb. *BioEssays* **24**, 460–465.

Cubbage CC, Mabee PM (1996) Development of the cranium and paired fins in the zebrafish *Danio rerio* (Ostariophysi, Cyprinidae). *J Morphol* **229**, 121–160.

Davis MC, Shubin NH, Force A (2004) Pectoral fin and girdle development in the basal actinopterygians *Polyodon spathula* and *Acipenser transmontanus*. *J Morphol* **262**, 608–628.

Dutel H, Herbin M, Clément G (2015) First occurrence of a mawsoniid coelacanth in the Early Jurassic of Europe. *J Vertebr Paleontol* **35**, e929581.

Dutel H, Galland M, Tafforeau P, et al. (2019) Neurocranial development of the coelacanth and the evolution of the sarcopterygian head. *Nature* **569**, 556–559.

Erdmann MV, Caldwell RL, Moosa MK (1998) Indonesian 'king of the sea' discovered. *Nature* **395**, 335.

Faustino M, Power DM (1999) Development of the pectoral, pelvic, dorsal and anal fins in cultured sea bream. *J Fish Biol* **54**, 1094–1110.

Forey PL (1981) The coelacanth *Rhabdoderma* in the Carboniferous of the British Isles. *Paleontology* **24**, 203–229.

Forey PL (1998) *History of the Coelacanth Fishes*. London: Chapman & Hall.

Fricke H, Hissmann K (1992) Locomotion, fin coordination and body form of the living coelacanth *Latimeria chalumnae*. *Environ Biol Fishes* **34**, 329–356.

Fricke H, Reinicke O, Hofer H, et al. (1987) Locomotion of the coelacanth *Latimeria chalumnae* in its natural environment. *Nature* **329**, 331–333.

Friedman M (2007) *Styloichthys* as the oldest coelacanth: Implications for early osteichthyan interrelationships. *J Syst Palaeontol* **5**, 289–343.

Friedman M, Brazeau MD (2010) A reappraisal of the origin and basal radiation of the Osteichthyes. *J Vertebr Paleontol* **30**, 36–56.

Friedman M, Coates MI (2006) A newly recognized fossil coelacanth highlights the early morphological diversification of the clade. *Proc R Soc B Biol Sci* **273**, 245–250.

Friedman M, Coates MI, Anderson P (2007) First discovery of a primitive coelacanth fin fills a major gap in the evolution of lobed fins and limbs. *Evol Dev* **9**, 329–337.

Gosline WA (1977) The structure and function of the dermal pectoral girdle in bony fishes with particular reference to ostariophysines. *J Zool* **183**, 329–338.

Grandel H, Schulte-Merker S (1998) The development of the paired fins in the zebrafish (*Danio rerio*). *Mech Dev* **79**, 99–120.

Gregory WK, Raven HC (1941) Part I: Paired Fins and Girdles in Ostracoderms, Placoderms, and Other Primitive Fishes. *Ann NY Acad Sci* **42**, 275–291.

Janvier P (1996) *Early vertebrates*. Oxford: Clarendon Press.

Jarvik E (1980) *Basic structure and evolution of vertebrates*. New York: Academic Press.

Johanson Z, Joss JM, Wood D (2004) The scapulocoracoid of the Queensland lungfish *Neoceratodus forsteri* (Dipnoi: Sarcopterygii): Morphology, development and evolutionary implications for bony fishes (Osteichthyes). *Zoology* **107**, 93–109.

Johanson Z, Long JA, Talent JA, et al. (2006) Oldest coelacanth, from the Early Devonian of Australia. *Biol Lett* **2**, 443–6.

Johanson Z, Joss J, Boisvert CA, et al. (2007) Fish fingers: digit homologues in sarcopterygian fish fins. *J Exp Zool B Mol Dev Evol* **308**, 757–768.

Jollie M (1980) Development of head and pectoral girdle skeleton and scales in *Acipenser*. *Copeia* **1980**, 226–249.

Joss J, Johanson Z (2007) Is *Palaeospondylus gunni* a fossil larval lungfish? Insights from *Neoceratodus forsteri* development. *J Exp Zool B Mol Dev Evol* **308**, 163–171.

Joss JM, Longhurst T (2001) Lungfish paired fins. In: *Major Events in Early Vertebrate Evolution* (ed Ahlberg PE), pp. 289–306. London: Taylor and Francis.

Jude E, Johanson Z, Kearsley A, et al. (2014) Early evolution of the lungfish pectoral-fin endoskeleton: evidence from the Middle Devonian (Givetian) *Pentlandia macroptera*. *Front Earth Sci* **2**, 1–15.

Koumoundouros G, Divanach P, Kentouri M (2001) Osteological development of *Dentex dentex* (osteichthyes: Sparidae): Dorsal, anal, paired fins and squamation. *Mar Biol* **138**, 399–406.

Lyckegaard A, Johnson G, Tafforeau P (2011) Correction of ring artifacts in X-ray tomographic images. *Int J Tomogr Simul* **18**, 1–9.

Mabee PM (2000) Developmental data and phylogenetic systematics: evolution of the vertebrate limb. *Am Zool* **40**, 789–800.

Mabee PM, Noordsy M (2004) Development of the paired fins in the paddlefish, *Polyodon spathula*. *J Morphol* **261**, 334–344.

Manzano A, Abdala V, Ponssa ML, et al. (2013) Ontogeny and tissue differentiation of the pelvic girdle and hind limbs of anurans. *Acta Zool* **94**, 420–436.

McGonnell IM (2001) The evolution of the pectoral girdle. *J Anat* **199**, 189–194.

Millot J, Anthony J (1958) *Anatomie de* Latimeria chalumnae*, Tome I: Squelette et Muscles*. Paris: CNRS.

Miyake T, Kumamoto M, Iwata M, et al. (2016) The pectoral fin muscles of the coelacanth *Latimeria chalumnae*: Functional and evolutionary implications for the fin-to-limb transition and subsequent evolution of tetrapods. *Anat Rec* **299**, 1203–1223.

Nagashima H, Kuraku S, Uchida K, et al. (2007) On the carapacial ridge in turtle embryos: its developmental origin, function and the chelonian body plan. *Development* **134**, 2219–2226.

Nakamura T, Gehrke AR, Lemberg J, et al. (2016) Digits and fin rays share common developmental histories. *Nature* **537**, 225–228.

Nowlan NC, Sharpe J (2014) Joint shape morphogenesis precedes cavitation of the developing hip joint. *J Anat* **224**, 482–489.

Nulens R, Scott L, Herbin M (2011) *An updated inventory of all known specimens of the coelacanth, Latimeria* spp. Grahamstown, South Africa: Smithiana Publ. Aquat. Biodivers.

Paganin D, Mayo SC, Gureyev TE, et al. (2002) Simultaneous phase and amplitude extraction from a single defocused image of a homogeneous object. *J Microsc* **206**, 33–40.

Patterson C (1982) Morphology and interrelationships of primitive actinopterygian fishes. *Integr Comp Biol* **22**, 241–259.

Pierce SE, Clack JA, Hutchinson JR (2012) Three-dimensional limb joint mobility in the early tetrapod *Ichthyostega*. *Nature* **486**, 523–526.

Pomikal C, Streicher J. (2010) 4D-analysis of early pelvic girdle development in the mouse (*Mus musculus*). *J Morphol* **271**(1), 116–126.

Pomikal C, Blumer R, Streicher J (2011) Four-dimensional analysis of early pelvic girdle development in *Rana temporaria*. *J Morphol* **272**, 287–301.

Pouyaud L, Wirjoatmodjo S, Rachmatika I, et al. (1999) A new species of coelacanth. *Life Sci* **322**, 261–267.

Rocková H, Rocek Z (2005) Development of the pelvis and posterior part of the vertebral column in the Anura. *J Anat* **206**, 17–35.

Rosen DE, Forey PL, Gardiner BG, et al. (1981) Lungfishes, tetrapods, paleontology, and plesiomorphy. *Bull Am Mus Nat Hist* **167**, 159–276.

Sanchez S, Ahlberg PE, Trinajstic KM, et al. (2012) Three-dimensional synchrotron virtual paleohistology: A new insight into the world of fossil bone microstructures. *Microsc Microanal* **18**, 1095–1105.

Schaeffer B (1941) A revision of *Coelacanthus newarki* and notes on the evolution of the girdles and basal plates of the median fins in the Coelacanthini. *Am Mus Novit* **1110**, 1–17.

Schaeffer B (1952) The Triassic coelacanth fish *Diplurus*, with observations on the evolution of the Coelacanthini. *Bull Am Mus Nat Hist* **99**, 25–78.

Shubin NH, Alberch P (1986) A morphogenetic approach to the origin and basic organization of the tetrapod limb. *Evol Biol* **20**, 319–387.

Shubin NH, Daeschler EB, Jenkins FAJ. (2006) The pectoral fin of *Tiktaalik roseae* and the origin of the tetrapod limb. *Nature* **440**, 764–771.

Smith JLB (1939) A living fish of mesozoic type. *Nature* **143**, 455–456.

Smith JLB (1956) *Old Fourlegs: the Story of the Coelacanth*. London: Longmans.

Standen EM, Du TY, Larsson HCE. (2014) Developmental plasticity and the origin of tetrapods. *Nature* **513**, 54–58.

Stensiö EA (1922) Über zwei Coelacanthiden aus dem Oberdevon von Wildungen. *Paläontol Z* **4**, 167–210.

Stensiö EA (1932) Triassic fishes from East Greenland: collected by the Danish expeditions in 1929–1931. *Medd Greenl* **83**, 1–305.

Vickaryous MK, Hall BK (2006) Homology of the reptilian coracoid and a reappraisal of the evolution and development of the amniote pectoral apparatus. *J Anat* **208**, 263–285.

Westoll TS (1943) The origin of the tetrapods. *Biol Rev* **18**, 78–98.

Zhu M, Schultze H-P (2001) Interrelationships of basal osteichthyans. In: *Major Events in Early Vertebrate Evolution* (ed. Ahlberg PE), pp. 289–306. London: Taylor and Francis.

Zhu M, Yu X (2009) Stem sarcopterygians have primitive polybasal fin articulation. *Biol Lett* **5**, 372–375.

Zhu M, Yu X, Choo B, et al. (2012a) Fossil fishes from China provide first evidence of dermal pelvic girdles in osteichthyans. *PLoS ONE* **7**, e35103.

Zhu M, Yu X, Lu J, et al. (2012b) Earliest known coelacanth skull extends the range of anatomically modern coelacanths to the Early Devonian. *Nat Commun* **3**, 772–778.

Supporting Information

Additional Supporting Information may be found in the online version of this article:

Fig. S1. *Latimeria chalumnae* – First pup. First (A, C) and second (B, D) mesomeres of the left pectoral fin in lateral view (A, B) and proximal view (C, D). The lateral view of the two mesomeres shows the different faces and the reorientation of the mesomeres along the axis. The proximal view shows the different articular surfaces of the first and second mesomeres. D = dorsal; L = lateral; M = medial; V= ventral. Not to scale.

Fig. S2. *Latimeria chalumnae* – Second pup. Transverse section of the distal end of the right fin (A) and its location on the lateral view of the 3D model (B). The distal radial presents only two convex faces, different from the previous axial elements of the fin that have four concave faces. dis.rad = distal radial; mes. = mesomere; po. acc. = post-axial accessory elements; pr. rad. = pre-axial radial. D = dorsal; L = lateral; M = medial; V= ventral. Not to scale.